**Article ID:** 1003－6326(2005)04－0913－09

# Effects of combination modes of favorable growth unit of $Al(OH)_3$ crystals precipitating on Van der Waals and chemical bond force①

WU Zheng-ping(吴争平), CHEN Qi-yuan(陈启元), YIN Zhou-lan(尹周澜), LI Jie(李 洁)
(School of Chemistry and Chemical Engineering, Central South University, Changsha 410083, China)

**Abstract:** The dipole moment, total energy, atomic charge, orbital population and orbital energy of four representative combination models of the favorable growth unit $Al_6(OH)_{18}(H_2O)_6$ of $Al(OH)_3$ crystals precipitating are calculated by *ab initio* at RHF/STO-3G, RHF/3-21G, RHF/6-31G levels and DFT at RB3LYP/STO-3G, RB3LYP/3-21G, RB3LYP/6-31G levels with Dipole & Sphere solvent model. The effect of various combination models on Van der Waals force is analyzed using dipole moment and molecular radius, and that on chemical bond force is analyzed using total energy, orbital population and orbital energy.

**Key words:** gibbsite; combination; *ab initio*; DFT; chemical bond force; Van der Waals force
**CLC number:** O 641.12 **Document code:** A

## 1 INTRODUCTION

A lot of studies on the crystallization of $Al(OH)_3$ from supersaturated sodium aluminate solution were carried out, but there are not many reports on the crystal strength[1-3]. The interrelated research indicated that strength of alumina was mainly related to strength of $Al(OH)_3$ precipitated from sodium aluminate solution[4, 5]. The nucleation, agglomeration and growth of $Al(OH)_3$ result in the combination of growth unit. Li et al[6-13] studied the structural characteristics of supersaturated sodium aluminate solution and growth units of $Al(OH)_3$ systematically. They brought forward and proved that the growth units of gibbsite were $Al(OH)_6^{3-}$ and $Al(OH)_6^{3-}$ polymer and $Al_6(OH)_{18}(H_2O)_6$ with hexagon face shape was the favorable growth unit.

On the base of the investigation by Li et al[6-13], the *ab intio* and DFT analyses on the structure of the favorable growth unit $Al_6(OH)_{18}(H_2O)_6$ were studied[14]. In this paper, effect of the combination mode of the favorable growth unit $Al_6(OH)_{18}(H_2O)_6$ on the Van der Waals and chemical bond force will be carried on.

## 2 CALCULATION METHODS AND THEORY

Based on *ab initio* Self Consistent Field molecular orbital theory and Density Function Theory method, the total energy, dipole moment, orbital population and atomic charge are calculated at STO-3G, 3-21G, 6-31G levels with Dipole & Sphere solvent model. Density Function Theory method adopts B3LYP Becke model with three parameters[15-17]. Calculations are performed at C2 workstation in Central South University by Gaussian98 program.

Based on the Molecular Mechanics Force Field, the geometry optimization is implemented by MM+ method using conjugation gradient Polak-Ribiere algorithm and the terminal condition is RMS gradient of 0.42 kJ/mol or the maximum cycles of 1 800.

Van der Waals force consists of action of inter moleculae. Although the force is quite infirm and the bond energy is very low, the physical properties such as boiling point, melting point, surface tension and viscosity, are influenced directly by this force. The orientation, abduction and dispersion forces are three kinds of Van der Waals force. Total Van der Waals action energy is[18]:

$$E = E_K + E_D + E_L = -\frac{2\mu_1^2 \cdot \mu_2^2}{3R^6kT} - \frac{\alpha_1\mu_1^2 + \alpha_2^2\mu_2^2}{R^6} - \frac{3}{2}\left[\frac{\alpha_1\alpha_2}{R^6}\right]\left[\frac{I_1I_2}{I_1 + I_2}\right] \quad (1)$$

where $E_K = -\frac{2\mu_1^2 \cdot \mu_2^2}{3R^6kT}$ is the orientation force (intermolecular average potential energy), $E_D =$

① **Foundation item:** Project(50374078) supported by the National Natural Science Foundation of China; Project(G1999064902) supported by the National Basic Research Program of China
**Received date:** 2004－04－20; **Accepted date:** 2004－12－30
**Correspondence:** WU Zheng-ping, PhD; Tel: +86-731-8877364-315; E-mail: wzp@mail.csu.edu.cn

$-\frac{\alpha_1\mu_1^2+\alpha_2^2\mu_2^2}{R^6}$ is the abduction force (intermolecular abduction action energy), $E_L=-\frac{3}{2}\left[\frac{\alpha_1\alpha_2}{R^6}\right]\cdot\left[\frac{I_1I_2}{I_1+I_2}\right]$ is the dispersion force (intermolecular attractable energy), $\mu$ is dipole moment, $R$ is intermolecular distance, $k$ is Boltzmann constant, $T$ is thermodynamics temperature, $\alpha$ is polarization rate, and $I$ is absolute value of ionization potential.

For the same molecular, total Van der Waals action energy is

$$E=E_K+E_D+E_L=-\frac{2\mu^4}{3R^6kT}-\frac{2\alpha_1\mu_1^2}{R^6}-\frac{3}{4}\frac{\alpha^2I}{R^6} \quad (2)$$

In this paper, two $Al_6(OH)_{18}(H_2O)_6$ units with four kinds of typical combination modes are studied, and the two $Al_6(OH)_{18}(H_2O)_6$ units are regarded as a large molecular system. Using parameters of dipole moment and molecular radius, the effect of various combination modes on Van der Waals force is analyzed.

## 3 COMBINATION MODES OF $Al_6(OH)_{18}(H_2O)_6$ AND CALCULATION MODEL

Four kinds of typical combination modes of the favorable growth unit $Al_6(OH)_{18}(H_2O)_6$ with hexagon face shape are designed. Regarding six Al as structure framework, there are side-uprightness-combination-A, side-face-combination-B, obverse-uprightness-combination-C and obverse-face-combination-D (Fig. 1). Fig. 2 shows the calculation models of four typical combination modes.

## 4 CALCULATION RESULTS AND DISCUSSION

### 4.1 Dipole moment and molecular radius

The molecular radius is calculated using Monte-Carlo method by *ab initio* and DFT at RHF/STO-3G, RHF/3-21G, RHF/6-31G, RB3LYP/STO-3G, RB3LYP/3-21G, RB3LYP/6-31G levels. Fig. 3 shows the calculated molecular radius. By the same methods of *ab initio* and DFT, using Self Consistent Field Onsager model, the dipole moment is calculated in the reaction field with dielectric constant of 78.39. Fig. 4 shows the calculated dipole moment.

Based on Equation (2), the orientation, inducement, and dispersion energies are proportional to quartic of dipole moment, square of polarization rate and dipole moment, square of polarization rate, respectively. The polarization rate is in direct proportion to cube of average molecular radius[18]. The molecular radii of four typical combination modes are nearly equal, and the difference is very small when calculating at 6-31G that is the most accurate level compared with STO-3G and 3-21G levels. Therefore, the difference of four systems' polarization rate is so small that it could be supposed that the polarization rate and intermolecular distance are equal approximately. Under this con-

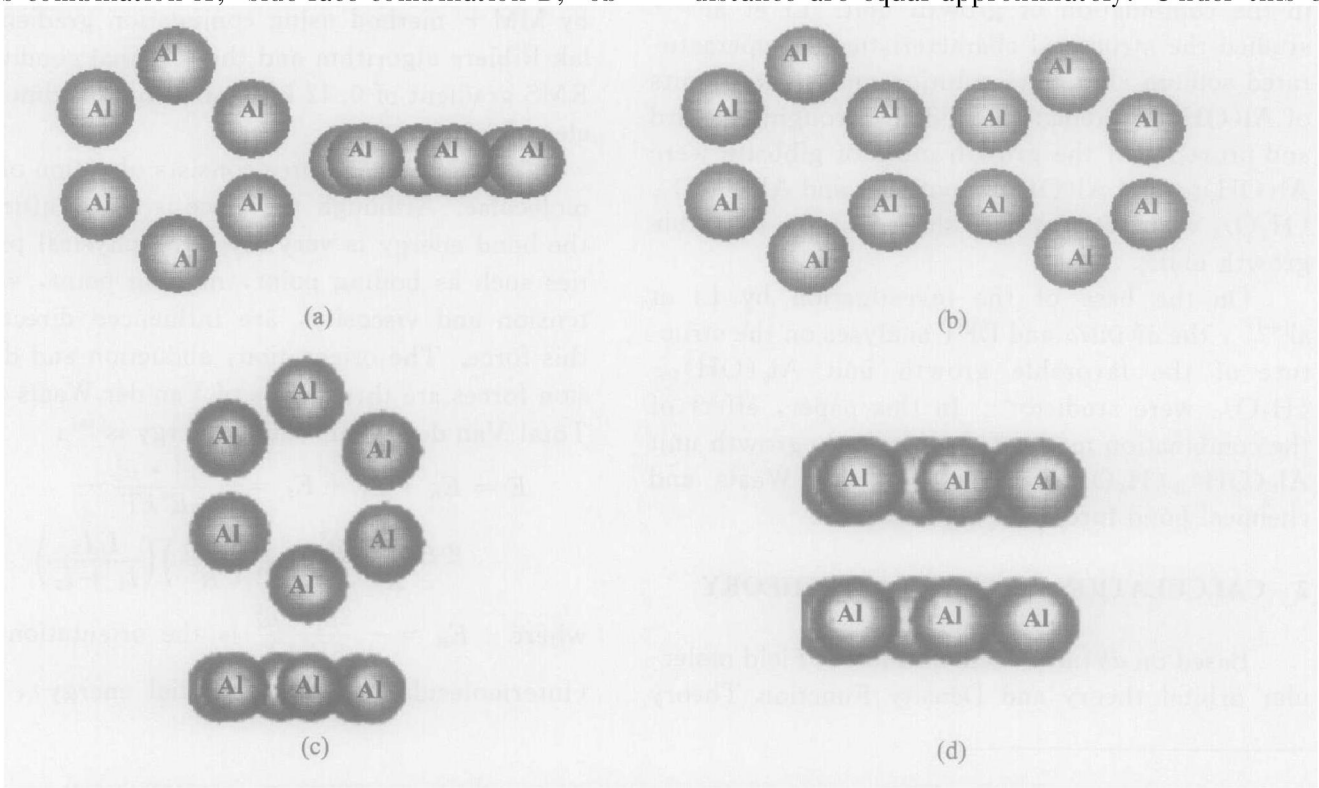


**Fig. 1** Sketch map of four combination modes of $Al_6(OH)_{18}(H_2O)_6$
(a) —Side-uprightness-combination-A; (b) —Side-face-combination-B;
(c) —Obverse-uprightness-combination-C; (d) —Obverse-face-combination-D

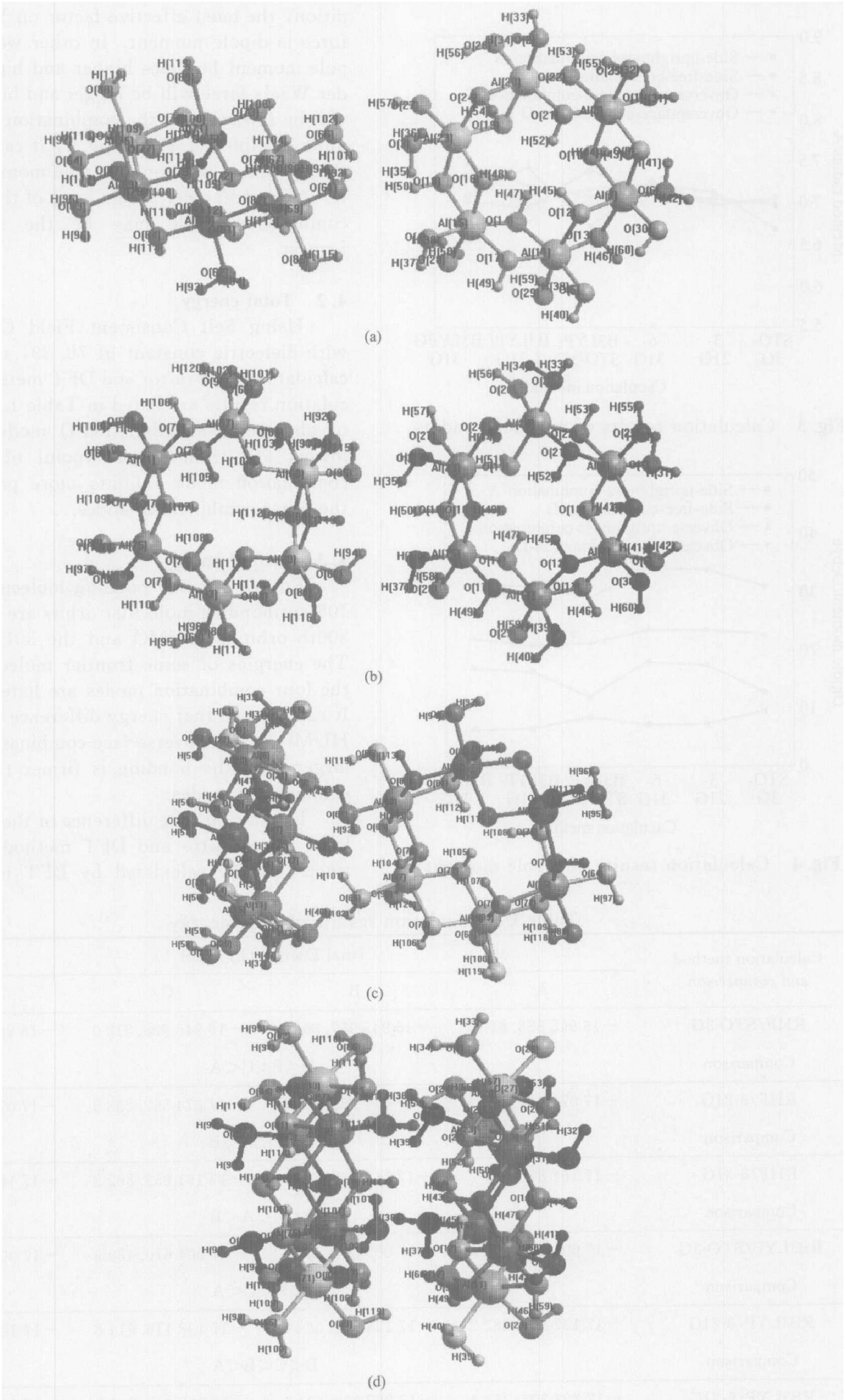

**Fig. 2** Calculation models for four combination modes of $Al_6(OH)_{18}(H_2O)_6$
(a) —Side-uprightness-combination-A; (b) —Side-face-combination-B;
(c) —Obverse-uprightness-combination-C; (d) —Obverse-face-combination-D

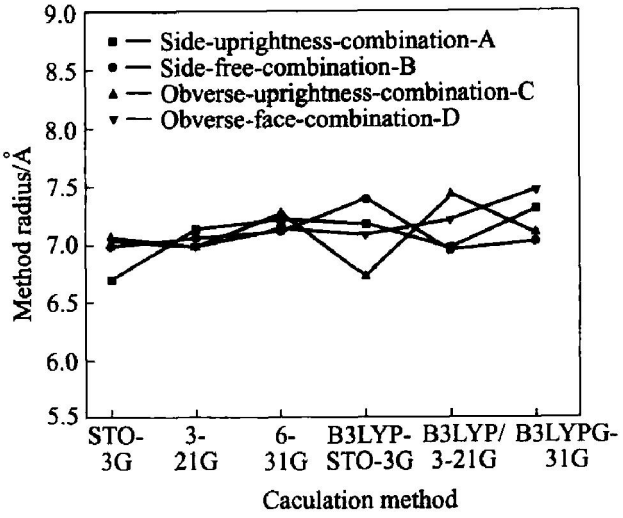


**Fig. 3** Calculation results of molecular radius

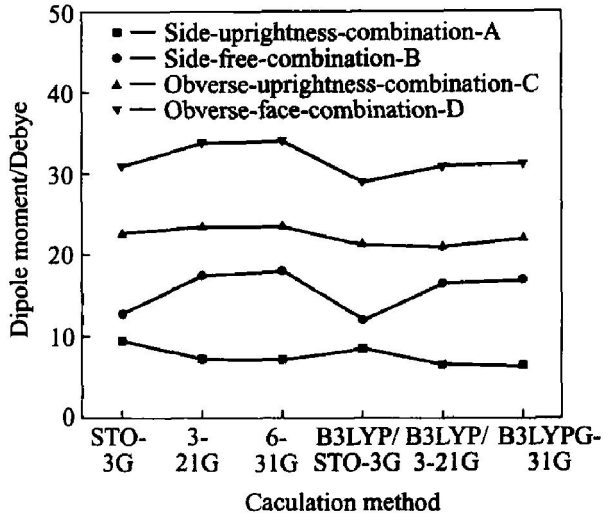


**Fig. 4** Calculation results of dipole moment

dition, the most effective factor on Van der Waals force is dipole moment. In other word, if the dipole moment becomes higher and higher, the Van der Waals force will be bigger and bigger, and this will be favorable to the combination of the growth units of gibbsite. From Fig. 4, it can be seen that the numerical relation of dipole moment is D> C> B> A, and Van der Waals force of the obverse-face combination mode may be the strongest and firmest.

### 4.2 Total energy

Using Self Consistent Field Onsager model with dielectric constant of 78.39, total energy is calculated by *ab initio* and DFT methods. The calculation results are listed in Table 1. Total energy of obverse-face-combination-D mode is relatively lower, and from the viewpoint of energy, this combination mode exhibits more possibility than the other combination modes.

### 4.3 Orbital energy

Energies of 300 bonding molecular orbits and 108 antibonding molecular orbits are acquired. The 300th orbit is HUMO and the 301st is LUMO. The energies of some frontier molecular orbits of the four combination modes are listed in Table 2. It can be seen that energy difference of LUMO and HUMO of the obverse-face-combination-D mode is larger, and the bonding is firmer than the other combination modes.

In addition, the difference of the results calculated by *ab initio* and DFT methods is very distinct. Energy calculated by DFT is higher than

**Table 1** Calculation results of total energy

| Calculation method and comparison | Total Energy/(kJ·mol$^{-1}$) | | | |
|---|---|---|---|---|
| | A | B | C | D |
| RHF/STO-3G | −16 945 858.817 6 | −16 945 957.806 6 | −16 945 908.512 0 | −16 946 104.003 0 |
| Comparison | D< B< C< A | | | |
| RHF/3-21G | −17 074 410.701 1 | −17 074 230.385 8 | −17 074 552.238 9 | −17 074 798.352 3 |
| Comparison | D< C< A< B | | | |
| RHF/6-31G | −17 161 870.709 2 | −17 161 675.775 7 | −17 161 952.862 2 | −17 162 149.812 7 |
| Comparison | D< C< A< B | | | |
| RB3LYP/STO-3G | −17 004 560.803 1 | −17 005 001.477 1 | −17 004 670.489 9 | −17 004 888.391 3 |
| Comparison | B< D< C< A | | | |
| RB3LYP/3-21G | −17 137 951.882 2 | −17 138 051.062 6 | −17 138 116.914 8 | −17 138 362.594 5 |
| Comparison | D< C< B< A | | | |
| RB3LYP/6-31G | −17 227 304.713 4 | −17 227 399.004 1 | −17 227 403.614 7 | −17 227 576.266 0 |
| Comparison | D< C< B< A | | | |

**Table 2** Calculation results of orbital energy $10^{-18}$ J

| Number of orbitals | Calculation method | | | | | |
|---|---|---|---|---|---|---|
| | RHF/STO-3G | RHF/3-21G | RHF/6-31G | RB3LYP/STO-3G | RB3LYP/3-21G | RB3LYP/6-31G |
| **Side-uprightness-combination-A** | | | | | | |
| 296 | - 0.848 276 | - 1.581 760 | - 1.688 051 | 0.083 445 | - 0.840 559 | - 0.945 193 |
| 297 | - 0.812 221 | - 1.568 332 | - 1.669 173 | 0.091 729 | - 0.822 902 | - 0.929 324 |
| 298 | - 0.798 515 | - 1.539 907 | - 1.643 913 | 0.128 482 | - 0.794 826 | - 0.899 721 |
| 299 | - 0.788 504 | - 1.519 023 | - 1.628 322 | 0.155 033 | - 0.762 999 | - 0.877 356 |
| 300(HOMO) | - 0.758 291 | - 1.430 346 | - 1.536 429 | 0.173 954 | - 0.684 960 | - 0.793 605 |
| 301(LOMO) | 1.696 290 | 0.400 656 | 0.243 909 | 0.759 512 | - 0.231 808 | - 0.340 228 |
| 302 | 1.795 083 | 0.540 173 | 0.381 828 | 0.889 868 | - 0.118 018 | - 0.232 244 |
| 303 | 1.873 209 | 0.578 015 | 0.412 694 | 0.936 299 | - 0.084 361 | - 0.201 508 |
| 304 | 1.945 843 | 0.650 867 | 0.470 940 | 0.970 577 | - 0.007 106 | - 0.129 350 |
| 305 | 2.019 261 | 0.695 554 | 0.501 327 | 1.049 915 | 0.023 848 | - 0.102 541 |
| LUMO-HOMO | 2.454 581 | 1.831 002 | 1.780 338 | 0.585 558 | 0.453 152 | 0.453 377 |
| **Side-face-combination-B** | | | | | | |
| 296 | - 0.787 806 | - 1.473 819 | - 1.595 013 | 0.131 206 | - 0.747 043 | - 0.855 644 |
| 297 | - 0.785 365 | - 1.474 380 | - 1.575 875 | 0.148 144 | - 0.730 476 | - 0.837 682 |
| 298 | - 0.751 010 | - 1.425 463 | - 1.530 359 | 0.163 534 | - 0.684 306 | - 0.793 823 |
| 299 | - 0.737 451 | - 1.391 850 | - 1.497 792 | 0.201 072 | - 0.661 592 | - 0.769 539 |
| 300(HOMO) | - 0.713 342 | - 1.365 996 | - 1.468 756 | 0.206 913 | - 0.635 956 | - 0.741 332 |
| 301(LOMO) | 1.726 765 | 0.466 406 | 0.316 997 | 0.842 994 | - 0.165 494 | - 0.277 672 |
| 302 | 1.780 608 | 0.526 004 | 0.367 134 | 0.855 339 | - 0.107 991 | - 0.224 135 |
| 303 | 1.792 162 | 0.543 312 | 0.378 034 | 0.862 053 | - 0.092 514 | - 0.213 366 |
| 304 | 1.851 367 | 0.595 280 | 0.431 746 | 0.922 043 | - 0.037 625 | - 0.156 995 |
| 305 | 1.966 900 | 0.641 537 | 0.471 943 | 0.999 777 | - 0.003 139 | - 0.130 270 |
| LUMO-HOMO | 2.440 107 | 1.832 402 | 1.785 753 | 0.636 081 | 0.470 462 | 0.463 660 |
| **Obverse-uprightness-combination-C** | | | | | | |
| 296 | - 0.831 099 | - 1.604 736 | - 1.716 738 | 0.047 216 | - 0.854 423 | - 0.957 444 |
| 297 | - 0.813 267 | - 1.551 809 | - 1.664 116 | 0.112 351 | - 0.827 655 | - 0.926 490 |

**Continue**

Obverse-uprightness-combination-C

| Number of orbitals | Calculation method | | | | | |
|---|---|---|---|---|---|---|
| | RHF/ STO-3G | RHF/ 3-21G | RHF/ 6-31G | RB3LYP/ STO-3G | RB3LYP/ 3-21G | RB3LYP/ 6-31G |
| 298 | - 0.801 540 | - 1.521 770 | - 1.640 399 | 0.155 425 | - 0.778 477 | - 0.880 713 |
| 299 | - 0.769 234 | - 1.481 660 | - 1.597 935 | 0.183 458 | - 0.748 133 | - 0.843 524 |
| 300(HOMO) | - 0.747 261 | - 1.414 172 | - 1.531 492 | 0.205 693 | - 0.675 935 | - 0.777 953 |
| 301(LOMO) | 1.623 788 | 0.325 804 | 0.160 657 | 0.721 756 | - 0.277 367 | - 0.409 816 |
| 302 | 1.821 546 | 0.512 227 | 0.362 862 | 0.871 644 | - 0.130 662 | - 0.260 582 |
| 303 | 1.881 537 | 0.536 293 | 0.366 916 | 0.928 539 | - 0.091 729 | - 0.226 271 |
| 304 | 1.908 305 | 0.612 065 | 0.445 523 | 0.978 633 | - 0.057 941 | - 0.168 504 |
| 305 | 1.947 761 | 0.639 183 | 0.463 092 | 0.993 587 | - 0.020 142 | - 0.144 656 |
| LUMO-HOMO | 2.371 049 | 1.739 976 | 1.686 742 | 0.516 063 | 0.398 568 | 0.368 137 |

Obverse-face-combination-D

| Number of orbitals | Calculation method | | | | | |
|---|---|---|---|---|---|---|
| | RHF/ STO-3G | RHF/ 3-21G | RHF/ 6-31G | RB3LYP/ STO-3G | RB3LYP/ 3-21G | RB3LYP/ 6-31G |
| 296 | - 0.812 047 | - 1.588 213 | - 1.694 547 | 0.077 037 | - 0.824 167 | - 0.931 896 |
| 297 | - 0.795 218 | - 1.578 011 | - 1.686 045 | 0.104 067 | - 0.812 831 | - 0.915 460 |
| 298 | - 0.768 362 | - 1.532 844 | - 1.634 426 | 0.180 319 | - 0.757 245 | - 0.856 255 |
| 299 | - 0.734 618 | - 1.509 432 | - 1.609 619 | 0.194 270 | - 0.731 871 | - 0.835 589 |
| 300(HOMO) | - 0.713 952 | - 1.449 180 | - 1.546 795 | 0.252 822 | - 0.669 963 | - 0.770 978 |
| 301(LOMO) | 1.745 600 | 0.476 302 | 0.315 907 | 0.834 412 | - 0.176 395 | - 0.291 667 |
| 302 | 1.802 756 | 0.518 200 | 0.344 202 | 0.871 993 | - 0.132 100 | - 0.250 947 |
| 303 | 1.938 518 | 0.635 041 | 0.469 632 | 0.985 434 | - 0.027 554 | - 0.156 995 |
| 304 | 1.993 756 | 0.678 726 | 0.523 170 | 1.057 762 | - 0.002 354 | - 0.119 414 |
| 305 | 2.070 750 | 0.745 168 | 0.541 306 | 1.098 613 | 0.071 805 | - 0.058 900 |
| LUMO-HOMO | 2.459 552 | 1.925 482 | 1.862 702 | 0.581 590 | 0.493 568 | 0.479 311 |
| Comparison | D> A> B> C | D> B> A> C | D> B> A> C | B> A> D> C | D> B> A> C | D> B> A> C |

that by *ab initio*. The reason for this is that on the base of Non-Relativity, Oppenheimer and Orbital Approximations, *ab intio* is a method of Hartree-Fock equation by Self Consistent Field, nevertheless, DFT is to use the electronic density to gain the properties of system.

### 4.4 Analysis of orbital population

Orbital populations of 708 bonding and anti-bonding orbits of four systems are calculated by *ab initio* and DFT methods at RHF/STO-3G, RHF/3-21G, RHF/6-31G, RB3LYP/STO-3G, RB3LYP/3-21G, RB3LYP/6-31G levels using Self Consistent Field Onsager model with dielectric constant of 78.39. Some orbital populations calculated at RHF/6-31G and RB3LYP/6-31G levels and the average populations of 3PX, 3PY, 3PZ orbits are listed in Table 3. It can be seen that except for Al 7 and Al 8, the numerical relation of 3S orbital population of the other ten Al is D> C> A>

**Table 3** Calculation results of some orbital populations

| No. Atom | Orbital number | Orbit | Orbital population | | | | | | | |
|---|---|---|---|---|---|---|---|---|---|---|
| | | | A | | B | | C | | D | |
| | | | RHF/6-31G | RB3LYP/6-31G | RHF/6-31G | RB3LYP/6-31G | RHF/6-31G | RB3LYP/6-31G | RHF/6-31G | RB3LYP/6-31G |
| 7 Al | 60 | 3S | 0.339 8 | 0.339 6 | 0.339 1 | 0.322 3 | 0.379 1 | 0.336 1 | 0.362 3 | 0.327 6 |
| | 61 | 3PX | 0.174 1 | 0.202 0 | 0.171 8 | 0.197 9 | 0.188 4 | 0.215 9 | 0.168 6 | 0.192 5 |
| | 62 | 3PY | 0.174 1 | 0.190 2 | 0.156 7 | 0.157 0 | 0.166 9 | 0.180 2 | 0.160 6 | 0.171 1 |
| | 63 | 3PZ | 0.158 2 | 0.178 6 | 0.165 9 | 0.190 2 | 0.164 4 | 0.192 9 | 0.197 6 | 0.223 5 |
| Average of 3PX, 3PY, 3PZ | | | 0.168 8 | 0.190 3 | 0.164 8 | 0.181 7 | 0.173 2 | 0.196 3 | 0.175 6 | 0.195 7 |
| 8 Al | 73 | 3S | 0.326 2 | 0.316 1 | 0.321 3 | 0.302 3 | 0.381 1 | 0.353 4 | 0.372 6 | 0.341 8 |
| | 74 | 3PX | 0.170 2 | 0.195 1 | 0.171 6 | 0.196 1 | 0.170 4 | 0.194 1 | 0.158 3 | 0.185 5 |
| | 75 | 3PY | 0.155 8 | 0.167 2 | 0.155 2 | 0.149 0 | 0.184 4 | 0.202 8 | 0.185 0 | 0.202 2 |
| | 76 | 3PZ | 0.183 8 | 0.212 3 | 0.160 3 | 0.186 6 | 0.166 7 | 0.195 3 | 0.189 3 | 0.213 9 |
| Average of 3PX, 3PY, 3PZ | | | 0.169 9 | 0.191 5 | 0.162 4 | 0.177 2 | 0.173 8 | 0.196 5 | 0.177 5 | 0.200 5 |
| 11 Al | 104 | 3S | 0.311 1 | 0.265 0 | 0.301 2 | 0.261 9 | 0.352 5 | 0.294 6 | 0.376 0 | 0.333 1 |
| | 105 | 3PX | 0.143 2 | 0.151 5 | 0.154 1 | 0.166 7 | 0.187 7 | 0.220 3 | 0.157 6 | 0.175 6 |
| | 106 | 3PY | 0.165 7 | 0.193 2 | 0.178 6 | 0.209 3 | 0.191 2 | 0.223 9 | 0.186 1 | 0.216 9 |
| | 107 | 3PZ | 0.196 3 | 0.227 1 | 0.168 9 | 0.193 5 | 0.132 3 | 0.132 4 | 0.169 7 | 0.183 0 |
| Average of 3PX, 3PY, 3PZ | | | 0.168 4 | 0.190 6 | 0.167 2 | 0.223 2 | 0.170 4 | 0.192 2 | 0.171 1 | 0.191 8 |
| 15 Al | 144 | 3S | 0.325 0 | 0.291 4 | 0.309 7 | 0.274 4 | 0.346 5 | 0.313 5 | 0.366 6 | 0.325 8 |
| | 145 | 3PX | 0.159 4 | 0.174 2 | 0.164 0 | 0.179 3 | 0.175 5 | 0.200 2 | 0.168 8 | 0.195 6 |
| | 146 | 3PY | 0.154 1 | 0.171 8 | 0.175 8 | 0.197 5 | 0.180 3 | 0.205 7 | 0.185 8 | 0.209 6 |
| | 147 | 3PZ | 0.192 1 | 0.223 6 | 0.173 1 | 0.199 3 | 0.158 4 | 0.177 2 | 0.182 4 | 0.203 8 |
| Average of 3PX, 3PY, 3PZ | | | 0.168 5 | 0.189 9 | 0.171 0 | 0.192 0 | 0.171 4 | 0.194 4 | 0.179 0 | 0.203 0 |
| 20 Al | 193 | 3S | 0.314 8 | 0.283 3 | 0.304 4 | 0.281 0 | 0.330 7 | 0.288 5 | 0.350 1 | 0.294 3 |
| | 194 | 3PX | 0.155 9 | 0.169 0 | 0.147 5 | 0.151 2 | 0.181 8 | 0.210 6 | 0.160 6 | 0.182 0 |
| | 195 | 3PY | 0.182 2 | 0.204 0 | 0.165 9 | 0.183 9 | 0.167 7 | 0.189 7 | 0.170 8 | 0.194 8 |
| | 196 | 3PZ | 0.154 3 | 0.182 2 | 0.169 8 | 0.198 1 | 0.151 1 | 0.166 0 | 0.179 9 | 0.204 4 |
| Average of 3PX, 3PY, 3PZ | | | 0.161 4 | 0.185 1 | 0.161 1 | 0.177 7 | 0.166 9 | 0.188 8 | 0.170 4 | 0.193 7 |
| 23 Al | 224 | 3S | 0.340 9 | 0.317 2 | 0.323 7 | 0.302 2 | 0.344 7 | 0.318 7 | 0.374 9 | 0.335 9 |
| | 225 | 3PX | 0.157 1 | 0.164 0 | 0.163 0 | 0.171 4 | 0.175 9 | 0.201 9 | 0.161 3 | 0.189 5 |
| | 226 | 3PY | 0.179 1 | 0.202 2 | 0.159 9 | 0.176 2 | 0.167 0 | 0.189 3 | 0.179 0 | 0.202 5 |
| | 227 | 3PZ | 0.162 4 | 0.185 8 | 0.168 3 | 0.195 6 | 0.145 4 | 0.158 0 | 0.174 7 | 0.189 2 |
| Average of 3PX, 3PY, 3PZ | | | 0.166 2 | 0.184 0 | 0.163 7 | 0.181 1 | 0.162 8 | 0.183 1 | 0.171 7 | 0.193 7 |
| 67 Al | 414 | 3S | 0.335 5 | 0.331 9 | 0.336 1 | 0.327 3 | 0.351 2 | 0.344 0 | 0.386 4 | 0.354 3 |
| | 415 | 3PX | 0.167 0 | 0.194 1 | 0.166 3 | 0.175 6 | 0.198 5 | 0.222 9 | 0.156 0 | 0.181 7 |
| | 416 | 3PY | 0.159 0 | 0.169 3 | 0.160 9 | 0.175 9 | 0.168 9 | 0.177 7 | 0.166 0 | 0.179 2 |
| | 417 | 3PZ | 0.183 7 | 0.209 7 | 0.164 7 | 0.191 2 | 0.180 1 | 0.206 8 | 0.197 1 | 0.226 8 |
| Average of 3PX, 3PY, 3PZ | | | 0.169 9 | 0.191 0 | 0.164 0 | 0.180 8 | 0.182 5 | 0.202 5 | 0.173 0 | 0.195 9 |

**Continue**

| No. Atom | Orbital number | Orbit | Orbital population | | | | | | | |
|---|---|---|---|---|---|---|---|---|---|---|
| | | | A | | B | | C | | D | |
| | | | RHF/ 6-31G | RB3LYP/ 6-31G | RHF/ 6-31G | RB3LYP/ 6-31G | RHF/ 6-31G | RB3LYP/ 6-31G | RHF/ 6-31G | RB3LYP/ 6-31G |
| 68 Al | 427 | 3S | 0.338 4 | 0.316 0 | 0.310 9 | 0.277 1 | 0.356 7 | 0.333 0 | 0.370 1 | 0.326 4 |
| | 428 | 3PX | 0.153 6 | 0.171 4 | 0.196 7 | 0.212 1 | 0.175 4 | 0.193 8 | 0.153 9 | 0.180 7 |
| | 429 | 3PY | 0.191 7 | 0.217 9 | 0.160 1 | 0.171 9 | 0.190 3 | 0.208 7 | 0.191 2 | 0.218 5 |
| | 430 | 3PZ | 0.159 0 | 0.174 3 | 0.159 9 | 0.181 6 | 0.174 3 | 0.197 6 | 0.181 7 | 0.196 2 |
| Average of 3PX, 3PY, 3PZ | | | 0.168 1 | 0.187 9 | 0.172 2 | 0.188 5 | 0.180 0 | 0.200 0 | 0.175 6 | 0.198 5 |
| 71 Al | 458 | 3S | 0.310 2 | 0.269 7 | 0.293 1 | 0.254 3 | 0.318 8 | 0.269 4 | 0.345 3 | 0.293 1 |
| | 459 | 3PX | 0.140 5 | 0.146 9 | 0.184 7 | 0.212 7 | 0.144 4 | 0.151 3 | 0.159 9 | 0.176 2 |
| | 460 | 3PY | 0.202 0 | 0.235 5 | 0.142 2 | 0.155 8 | 0.183 5 | 0.214 2 | 0.189 0 | 0.219 3 |
| | 461 | 3PZ | 0.160 4 | 0.187 2 | 0.168 9 | 0.194 2 | 0.178 2 | 0.206 3 | 0.176 1 | 0.198 4 |
| Average of 3PX, 3PY, 3PZ | | | 0.167 6 | 0.189 9 | 0.165 3 | 0.187 6 | 0.168 7 | 0.190 6 | 0.175 0 | 0.198 0 |
| 75 Al | 498 | 3S | 0.324 8 | 0.291 1 | 0.302 0 | 0.268 1 | 0.330 3 | 0.300 3 | 0.388 2 | 0.349 8 |
| | 499 | 3PX | 0.154 8 | 0.175 7 | 0.184 8 | 0.217 6 | 0.162 4 | 0.187 1 | 0.179 9 | 0.208 8 |
| | 500 | 3PY | 0.196 7 | 0.227 6 | 0.140 8 | 0.149 4 | 0.166 8 | 0.184 0 | 0.176 1 | 0.196 3 |
| | 501 | 3PZ | 0.158 6 | 0.175 2 | 0.171 0 | 0.196 9 | 0.179 1 | 0.204 7 | 0.170 3 | 0.190 0 |
| Average of 3PX, 3PY, 3PZ | | | 0.170 0 | 0.192 8 | 0.165 5 | 0.188 0 | 0.169 4 | 0.191 9 | 0.175 4 | 0.198 3 |
| 80 Al | 547 | 3S | 0.324 8 | 0.303 5 | 0.310 3 | 0.280 4 | 0.332 3 | 0.313 0 | 0.383 7 | 0.352 9 |
| | 548 | 3PX | 0.145 0 | 0.160 8 | 0.157 6 | 0.168 2 | 0.145 9 | 0.163 2 | 0.162 5 | 0.185 9 |
| | 549 | 3PY | 0.148 5 | 0.171 3 | 0.159 5 | 0.173 5 | 0.166 0 | 0.185 3 | 0.161 8 | 0.182 3 |
| | 550 | 3PZ | 0.182 5 | 0.205 8 | 0.173 1 | 0.200 5 | 0.165 8 | 0.191 6 | 0.176 2 | 0.190 8 |
| Average of 3PX, 3PY, 3PZ | | | 0.158 7 | 0.179 3 | 0.163 4 | 0.180 7 | 0.159 2 | 0.180 0 | 0.166 8 | 0.186 3 |
| 83 Al | 578 | 3S | 0.329 0 | 0.307 2 | 0.323 4 | 0.300 9 | 0.331 1 | 0.310 2 | 0.370 2 | 0.342 6 |
| | 579 | 3PX | 0.142 3 | 0.156 6 | 0.141 9 | 0.145 3 | 0.140 6 | 0.153 8 | 0.163 3 | 0.191 5 |
| | 580 | 3PY | 0.153 6 | 0.172 9 | 0.168 0 | 0.191 1 | 0.170 7 | 0.194 5 | 0.170 8 | 0.189 6 |
| | 581 | 3PZ | 0.183 6 | 0.211 3 | 0.168 9 | 0.195 0 | 0.172 1 | 0.196 4 | 0.172 2 | 0.185 6 |
| Average of 3PX, 3PY, 3PZ | | | 0.159 8 | 0.180 2 | 0.159 6 | 0.177 1 | 0.161 1 | 0.181 6 | 0.168 8 | 0.188 9 |

B, and 3PX, 3PY, 3PZ orbital average population of the obverse-face-combination-D is the largest. The calculation results show that the bonding of the obverse-face-combination-D mode is firmer than the other combination modes.

The calculation results of total energy, atomic charge, orbital population and orbital energy all accord with the prediction about bonding orientation of the favorable growth unit $Al_6(OH)_{18}(H_2O)_6$ in Ref. [14].

## 5 CONCLUSIONS

1) The calculation results of dipole moment and molecular radius speculate that Van der Waals force of the obverse-face combination mode is the strongest and the firmest, and this combination mode seems more possible than the others.

2) The calculation results of total energy, orbital population and orbital energy indicate that the

bonding of the obverse-face combination mode is the firmest because of the lower total energy, the largest energy difference of LUMO and HUMO and the higher orbital average populations.

## REFERENCES


[1] Sang J V. Factors affecting the attrition strength of alumina products[J]. Light Metals, 1987, 2: 121 - 127.

[2] Stahlin W. Alumina morphology and particle strength [J]. Light Metals, 1985, 4: 423 - 432.

[3] Sweegers C. Morphology, evolution and other characteristics of gibbsite crystals grown from pure and impure aqueous sodium aluminate solutions[J]. Journal of Crystal Growth, 2001, 233(3): 567 - 582.

[4] Frances C. Particle morphology of ground gibbsite in different grinding environments[J]. Mineral Processing, 2001, 6(1): 41 - 56.

[5] Belaroui K. Morphological characterization of gibbsite and alumina[J]. Powder Technology, 2002, 127(2): 246 - 256.

[6] LI Jie. Study on the structure characteristics and decomposition mechanism of supersaturated sodium aluminate solution[D]. Changsha: Central South University, 2001. 12. (in Chinese)

[7] LI Jie, CHEN Qi-yuan. Investigation on the mode of the growth unit for alumina trihydrate crystals precipitation from supersaturated sodium aluminate solution [A]. Hydrometallurgy, ICHM'98 [C]. Kunming, China, 1998. 240.

[8] LI Jie, CHEN Qi-yuan, YIN Zhou-lan. Studies on the kinetics of unseeded nucleation of aluminum trihydroxide from supersaturated sodium aluminate solutions [J]. Chemical Journal of Chinese University, 2003, 24 (9): 1652 - 1656. (in Chinese)

[9] LI Jie, CHEN Qi-yuan, YIN Zhou-lan, et al. Development and prospect in the fundamental research on the decomposition of supersaturated sodium aluminate solution[J]. Progress in Chemistry, 2003, 15(3): 170 - 177. (in Chinese)

[10] CHEN Qi-yuan, LI Jie, YIN Zhou-lan, et al. Decomposition of supersaturated sodium aluminate solution[J]. Trans Nonferrous Metals Soc China, 2003, 13(3): 649 - 654.

[11] CHEN Qi-yuan, ZHOU Jun, LI Jie, et al. A theoretical investigation on the transformation of aluminate ions[J]. Trans Nonferrous Metals Soc China, 2003, 13(4): 812 - 818.

[12] CHEN Guo-hui, CHEN Qi-yuan, YIN Zhou-lan, et al. SEM observation of gibbsite precipitation with seeds from sodium aluminate solutions promoted by ultrasound[J]. Trans Nonferrous Met Soc China, 2003, 13(3): 708 - 714.

[13] LI Jie, CHEN Qi-yuan, YIN Zhou-lan, et al. Influence of supersaturation on the structure of sodium aluminate solutions with mediate concentration: a solution X-ray diffraction study[J]. Trans Nonferrous Met Soc China, 2002, 12(5): 992 - 996.

[14] WU Zheng-ping, CHEN Qi-yuan, YIN Zhou-lan, et al. Studies on the structure and bonding orientation of the favorable growth unit $Al_6(OH)_{18}(H_2O)_6$ of Gibbsite[J]. Trans Nonferrous Metals Soc China, (in press)

[15] Frisch M J, Trucks C W, Schlegel H W, et al. Gaussian98 [M]. Gaussian Inc, Pittshurgh PA, 1998.

[16] Wada K, Masui R, Matsubara H, et al. Properties and structure of the soluble ferredoxin from Synechococcus 6301 (Anacystis nidulans), Relationship to gene sequences [J]. J Biochem, 1988, 252(2): 571 - 575.

[17] Becke A D. Density-functional exchange-energy approximation with correct asymptotic behavior[J]. Phys Rev A, 1988, 38(9): 3098 - 3100.

[18] DENG Neng-wu, ZHANG Hong-lie, ZHAO Wei-rong. Physical Conception of Chemical Bond[M]. An Hui Technology Publishing Press, 1985. 199 - 208. (in Chinese)


**(Edited by YANG Bing)**